Strain pattern of each ligamentous band of the superficial deltoid ligament

Masato Takao (mmmmtakaooo@gmail.com)
Clinical and Research Institute for Foot and Ankle Surgery https://orcid.org/0000-0003-1186-7745
Satoru Ozeki
Dokkyo Ika Daigaku Saitama Iryo Center
Xavier Martin Oliva
Universitat de Barcelona
Ryota Inokuchi
Clinical and Research Institute for Foot and Ankle Surgery
Takayuki Yamazaki
Dokkyo Ika Daigaku Saitama Iryo Center
Yoshitaka Takeuchi
Tokyo National College of Technology
Maya Kubo
Teikyo Daigaku
Danielle Lowe
Lions Gate Hospital
Kentaro Matsui
Teikyo Daigaku
Mai Katakura
Clinical and Research Institute for Foot and Ankle Surgery
Mark Glazebrook
Dalhousie University

Research article

Keywords: tibionavicular ligament, tibiospring ligament, tibiocalcaneal ligament, superficial posterior tibiotalar ligament

Posted Date: February 10th, 2020

DOI: https://doi.org/10.21203/rs.2.22971/v1

Version of Record: A version of this preprint was published at BMC Musculoskeletal Disorders on May 9th, 2020. See the published version at https://doi.org/10.1186/s12891-020-03296-0.

Abstract

Background

There are few reports in terms of detailed biomechanics of the deltoid ligament, and no reports have measured the biomechanics of each ligamentous band, due to the difficulty in inserting sensors into the narrow ligaments. This study aims to measure the strain pattern of the deltoid ligament bands using a miniaturization ligament performance probe (MLPP) system.

Methods

The MLPP was sutured into the ligamentous bands of the deltoid ligament in 6 fresh-frozen lower extremity cadaveric specimens. The strain was measured using a round metal disk (clock) fixed on the plantar aspect of the foot. The ankle was manually moved from 15° of dorsiflexion to 30° plantar flexion, and a 1.2-N-m force was applied to the ankle and subtalar joint complex. The clock was then rotated every 30° to measure the strain of each ligamentous band at each endpoint.

Results

The tibionavicular ligament (TNL) begins to tense at 10° plantar flexion and the tension becomes stronger as the angle increases; the TNL works most effectively in plantar flex-abduction. The tibiospring ligament (TSL) begins to tense gradually at 15° plantar flexion and the tension becomes stronger as the angle increases. The TSL works most effectively in the abduction. The tibiocalcaneal ligament (TCL) begins to tense gradually at 0° dorsiflexion, and the tension becomes stronger as the angle increases. The TCL works most effectively in pronation (dorsiflexion-abduction). The superficial posterior tibiotalar ligament (SPTTL) begins to tense gradually at 0° dorsiflexion, and the tension becomes stronger as the angle increases, with the SPTTL working most effectively in dorsiflexion.

Conclusion

Our results provide a better understanding of the biomechanical function of the superficial deltoid ligament and could help in improving repair and reconstruction procedures.

Background

The deltoid ligament has both superficial and deep layers consisting of up to six ligamentous bands [15]. The superficial layer of the deltoid ligament is composed of four ligamentous bands, including the tibionavicular (TNL), tibiospring (TSL), tibiocalcaneal (TCL), and superficial posterior tibiotalar (SPTTL) ligaments. Two ligamentous bands make up the deep layer of the deltoid ligament: the deep anterior and posterior tibiotalar ligaments. Generally, the deltoid ligament is known to work cooperatively and is primarily responsible for 1) stabilizing the medial side of the ankle to limit anterior, posterior, and lateral translation of the talus and 2) restraining talar abduction at the talocrural joint [2, 6]. Specifically, the

superficial deltoid resists eversion of the hindfoot and the deep deltoid is the primary restraint to external rotation of the talus [5, 7, 8, 9].

There are few reports in terms of detailed biomechanics of the deltoid ligament [11, 16, 18, 19, 20], and no reports have measured the biomechanics of each ligamentous band, due to the difficulty in inserting sensors into the narrow ligaments. The paucity of biomechanics data regarding each ligamentous band may have contributed to less reliable results of secondary repairs or reconstructions of the deltoid ligament. Thus, clarifying the biomechanics of each ligamentous band of the deltoid ligament is crucial for designing and performing repair and reconstruction procedures.

In this study, we used a developed Miniaturization Ligament Performance Probe (MLPP) system that can be inserted into small ligaments to allow for the precise measurement of the strain patterns of the deltoid ligament during ankle motion.

Methods

MLPP system

The MLPP system is composed of a strain gauge (force probe), an amplifier unit, a display unit, and a logger (Fig. 1). This system is capable of detecting small changes in resistance on the force probe. These changes in resistance are then enlarged by the bridge of an amplifier unit and transferred to the input of the display unit. After analogue-to-digital conversion in the display unit, the amount of strain is displayed. This strain measurement is converted to analogue, and its voltage is finally recorded in the logger.

The force probe (Showa unilateral strain gauge; Showa Measuring Instruments Inc., Tokyo, Japan) is rectangular shaped (width, 1.4 mm; height, 1.4 mm; length, 8 mm) and has a tubular structure with slits entering vertically on one side of its surface (Fig. 2A). When strain is applied to the force probe, the internal strain gauge is distorted, allowing the magnitude of strain to be measured. When the force probe is inserted into the tissue, it may rotate as forces are applied causing the output to be reduced or inverted. To suppress this rotational influence, a tube was attached to the force probe, and both ends were sutured to the tissue to be measured (Fig. 2B).

A performance cube was used to measure the position of the ankle (Fig. 3). The cube is composed of an MPU-9250 motion processing sensor with a nine-axis sensor, an ESP32 microcontroller, and a logger. The MPU-9250 and ESP32 are loaded in the performance cube. The MPU-9250 is a sensor that acquires position information and can acquire values of motion in nine axes in total, each with angular acceleration, and geomagnetism. The MPU-9250 is equipped with hardware called a digital motion processor, which automatically measures at the time of initialization of the sensor and calculates posture. The ESP32 is a microcontroller that calculates data obtained from the MPU-9250 and transmits data to the logger via a WiFi module. This performance cube is synchronized with the MLPP system.

Cadaveric tests using the MLPP system

Six fresh-frozen through-the-knee lower extremity cadaveric specimens were used for this study (three right and three left). Three specimens were from male, and three were from female. The median age was 64 years (range 46–82 years). These specimens were free of ankle or hind foot deformities, did not undergo surgery or dissection, and did not have any history of trauma or other pathology that may alter the anatomy. All cadaveric studies were performed at University of Barcelona in Catalonia, Spain. All methods in this study were reviewed and approved by the institutional review board of The University of Barcelona. Consent for the storage and use of the bodies for research purposes was given by all body donors prior to death or by their next of kin.

Experiments on strain patterns of the superficial deltoid ligament

The following procedures were performed in all specimens by a single experienced foot and ankle surgeon. An incision was made in the medial ankle and the superficial layer of the deltoid ligament was exposed. Lines were drawn on ligaments to trace each ligament from its origin to insertion on the bone (Fig. 4A). Ligaments were not isolated to allow investigation as one unit. A force probe was placed in the mid-substance of each ligamentous band of the TNL, TSL, TCL, and SPTTL such that the slit of the force probe was aligned with the long axis of the ligament fibres (Fig. 4B). After introducing the force probe into the ligament, the force probe tube was sutured to the ligament fibres with 3 – 0 nylon thread to prevent the rotation of the force probe.

An Ilizarov ring-shaped external fixator was placed on the lower leg, and the lower limb was fixed vertically to the measurement desk using a vise to allow for the localization of the distal upper and proximal lower portions of the specimens. A round metal disk (clock, diameter 150 mm) with a 6-mm diameter hole every 30°, was affixed to an acrylic plate (width, 120 mm; length, 280 mm; thickness, 10 mm). This was fixed on the plantar aspect of the foot with a screw (diameter 6 mm) inserted to the calcaneus and a rod (diameter 8 mm) inserted between the second and third metatarsals (Fig. 3). This plate had a 25-cm arm where a 0.5-kg weight could be added at the end, applying a 1.2-N m force to the ankle and subtalar joint complex (0.5 kg × 0.25 m × 9.80665 = 1.2258312 N m). This arm was rotated every 30° on the clock to allow measurement of the strain on each ligamentous band at various ankle positions. The ankle positions were defined as dorsiflexion with the arm at the 12 o'clock position, plantar flexion at the 6 o'clock position, inversion at the 3 o'clock position, and eversion at 9 o'clock position; 1 and 2 o'clock defined dorsiflexion-adduction, 4 and 5 angle defined supination (plantar flexion adduction), 7 and 8 o'clock defined plantarflexion- abduction, and 10 and 11 o'clock defined pronation (dorsiflexion-abduction).

After the investigation of strain in the designated ankle positions, the strain values of each ligament was also measured in axial motion of the ankle from maximal dorsiflexion to plantar flexion.

The angles of axial, sagittal and horizontal motions were measured by an electronic goniometer (MPU-9250; TDK InvenSense) synchronized to the MLPP system.

Data analysis

The relationship between the foot positions and the tensile forces of each ligamentous band was analysed. The tensile force data from the force probe was obtained by synchronizing to the arm of the clock rotating every 30° and moving the ankle from 15° dorsiflexion to 30° plantar flexion 10 times manually and the strain of each ligamentous band during ankle motion was measured. Individual strain data were aligned to the value at neutral position (0) and to the maximum value (100). The average value at each position was connected by a line, and the ligament tension pattern was compared among the specimens.

Results

Tibionavicular ligament

The TNL was under the most strain in plantarflexion-abduction (Fig. 5A). The TNL began to tense gradually at 10° plantarflexion. The strain became stronger as the plantarflexion angle increased a maximum strain of 100 at 30° plantarflexion (Fig. 5B).

Tibiospring ligament

The TSL was under the most strain in eversion (Fig. 6A). The TSL began to tense gradually at 15° plantarflexion. The strain became stronger as the plantarflexion angle increased a maximum strain of 100 at 30° plantarflexion (Fig. 6B).

Tibiocalcaneal ligament

The TCL was under the most strain in pronation (Fig. 7A). The TCL began to tense gradually at 0° dorsiflexion. The strain became stronger as the dorsiflexion angle increased a maximum strain of 100 at 15° dorsiflexion (Fig. 7B).

Superficial posterior tibiotalar ligament

The SPTTL was under the most strain in dorsiflexion (Fig. 8A). The SPTTL began to tense gradually at 0° dorsiflexion. The strain became stronger as the dorsiflexion angle increased a maximum strain of 100 at 15° dorsiflexion (Fig. 8B).

Discussion

Understanding the biomechanical properties of each individual ligament in the ankle is of great importance. In this study, we gained a comprehensive understanding of the contribution of each ligamentous band in the deltoid ligament to overall ankle stability at various ankle positions.

Previous studies have evaluated biomechanics by 1) using a laboratory reference axis system to obtain a three-plane description of movements [13], 2) after sectioning of each ligamentous band [7], 3) by using reluctance transducers to measure deltoid ligament length change [16], 4) by using computational models [18], and 5) a marker-based motion analysis [19]. This is the first study in which each ligamentous band of the deltoid has been investigated without transection. This will allow for a more precise surgical repair or reconstruction after deltoid ligament injuries.

Numerous ligament reconstruction techniques have been proposed; however, clear indications for operative repair have not yet been well established. Some studies have shown that repair of the ruptured ligament is beneficial and can produce satisfactory results [11, 12, 14, 20]. By contrast, other studies showed repair of the deltoid ligament to be unnecessary [1, 4, 10, 17, 21]. There may be some advantages of adding deltoid ligament repair for patients with high fibular fractures or in patients with concomitant syndesmotic injury and fixation [3], but previous studies did not evaluate each ligamentous band by physical examination before surgery. In this study, we clarified the biomechanics of each ligamentous band of the deltoid ligament. This will allow for detailed preoperative assessment of ligament damage and adaptation of operative techniques and procedures, possibly leading to established indicators for operation.

Limitations

The disadvantage of MLPP is that it measures the strain value of the ligament instead of tensile force. In the elastic range where the deltoid ligament can return to its original shape and length, force and strain showed a linear proportional relationship. Therefore, it is theoretically possible to convert the measured strain value to newton-force if the Young's modulus is obtained by calibration. However, it is difficult to accurately determine the Young's modulus because the water content of the tissue decreases with time and the elasticity of the ligaments changes. The acceptable variation in the results of this study might be influenced by temporal changes in the elasticity of the ligaments.

Conclusion

We demonstrated biomechanical properties of each ligamentous band of the superficial layer of the deltoid ligament. These findings provide a better understanding of the biomechanical function of deltoid ligament, which could help in informing repair and reconstruction procedures.

Abbreviations

MLPP
Miniaturization Ligament Performance Probe
SPTTL
Superficial posterior tibiotalar ligament
TCL

Tibiocalcaneal ligament
TNL
Tibionavicular ligament
TSL
Tibiospring ligament

Declarations

Ethics approval and consent to participate

This study was a cadaveric study and approved according to the bylaws of the Bioethics Committee of the "Unitat d' Anatomia i Embriologia humana" of the Faculty of Medicine, University of Barcelona, Spain (Campus Clinic).

Consent for publication

Not applicable.

Availability of data and materials

The datasets used and/or analyzed during the current study are available from the corresponding author on reasonable request.

Competing interests

The authors declare that they have no competing interests.

Funding

All authors have no financial relationships relevant to this article to disclose.

Authors' contributions

MT, SO, XO, and MG designed the study, MT, SO, XO, TY, YT, MK, DL, KM, MK, and MG performed the research, RI wrote the first draft. All authors read and approved the final manuscript.

Acknowledgments

Not applicable.

References

1. Baird RA, Jackson ST. Fractures of the distal part of the fibula with associated disruption of the deltoid ligament. Treatment without repair of the deltoid ligament. J Bone Joint Surg Am 1987;69:1346-52.
2. Cromeens BP, Kirchhoff CA, Patterson RM, Motley T, Stewart D, Fisher C, et al. An attachment-based description of the medial collateral and spring ligament complexes. Foot Ankle Int 2015;36:710.
3. Dabash S, Elabd A, Potter E, Fernandez I, Gerzina C, Thabet AM, et al. Adding deltoid ligament repair in ankle fracture treatment: Is it necessary? A systematic review 2018;18:30223-6.
4. De Souza L, Gustilo RB, Meyer TJ. Results of operative treatment of displaced external rotation-abduction fractures of the ankle. JBJS 1985;67:1066.
5. Earll M, Wayne J, Brodrick C, Vokshoor A, and Adelaar R. Contribution of the deltoid ligament to ankle joint contact characteristics: a cadaver study. Foot Ankle Int. 1996;17:317-24.
6. Brodell JD Jr, MacDonald A, Perkins JA, Deland JT, and Oh I. Reconstruction of the deltoid-spring ligament: tibiocalcaneonavicular ligament complex. Tech Foot Ankle Surg 2016;15:39-46.
7. Harper MC. An anatomic study of the short oblique fracture of the distal fibula and ankle stability. Foot Ankle. 1983;4:23-9.
8. Harper MC. Deltoid ligament: an anatomical evaluation of function. Foot Ankle. 1987;8:19-22.
9. Harper MC. The deltoid ligament. An evaluation of need for surgical repair. Clin Orthop Relat Res. 1988;226:156-68.
10. Harper MC. Deltoid ligament: an anatomical evaluation of function. Foot Ankle 1987;8:19-22.
11. Hsu AR, Lareau CR, and Anderson RB. Repair of acute superficial deltoid complex avulsion during ankle fracture fixation in National Football League players. Foot Ankle Int 2015;36:1272-8.
12. Johnson D and Hill J. Fracture-dislocation of the ankle with rupture of the deltoid ligament. Injury 1988;19:59-61.
13. Kjaersgaard-Andersen P, Wethelund JO, Helmig P, and Søballe K. Stabilizing effect of the tibiocalcaneal fascicle of the deltoid ligament on hindfoot joint movements: an experimental study. Foot Ankle. 1989;10:30-5.
14. Little MM, Berkes MB, Schottel PC, Garner MR, Lazaro LE, Birnbaum JF, et al. Anatomic fixation of supination external rotation type IV equivalent ankle fractures. J Orthop Trauma 2015;29:250-5.

15. Pankovich AM and Shivaram MS. Anatomical basis of variability in injuries of the medial malleolus and the deltoid ligament. I. Anatomical studies. Acta Orthop Scand. 1979;50:217-23.
16. Tochigi Y, Rudert MJ, Amendola A, Brown TD, and Saltzman CL. Tensile engagement of the peri-ankle ligaments in stance phase. Foot Ankle Int. 2005;26:1067-73.
17. Tourne Y, Charbel A, Picard F, Montbarbon E, and Saragaglia D. Surgical treatment of bi-and trimalleolar ankle fractures: should the medial collateral ligament be sutured or not? J Foot Ankle Surg 1999;38:24-9.
18. Wei F, Hunley SC, Powell JW, and Haut RC. Development and validation of a computational model to study the effect of foot constraint on ankle injury due to external rotation. Ann Biomed Eng. 2011;39:756-65.
19. Wei F, Braman JE, Weaver BT, and Haut RC. Determination of dynamic ankle ligament strains from a computational model driven by motion analysis based kinematic data. J Biomech. 2011;44:2636-41.
20. Yu GR, Zhang MZ, Aiyer A, Tang X, Xie M, Zeng LR, et al. Repair of the acute deltoid ligament complex rupture associated with ankle fractures: a multicenter clinical study. J Foot Ankle Surg 2015;54:198-202.
21. Zeegers AV and van der Werken C. Rupture of the deltoid ligament in ankle fractures: should it be repaired? Injury 1989;20:39-41.

Figures

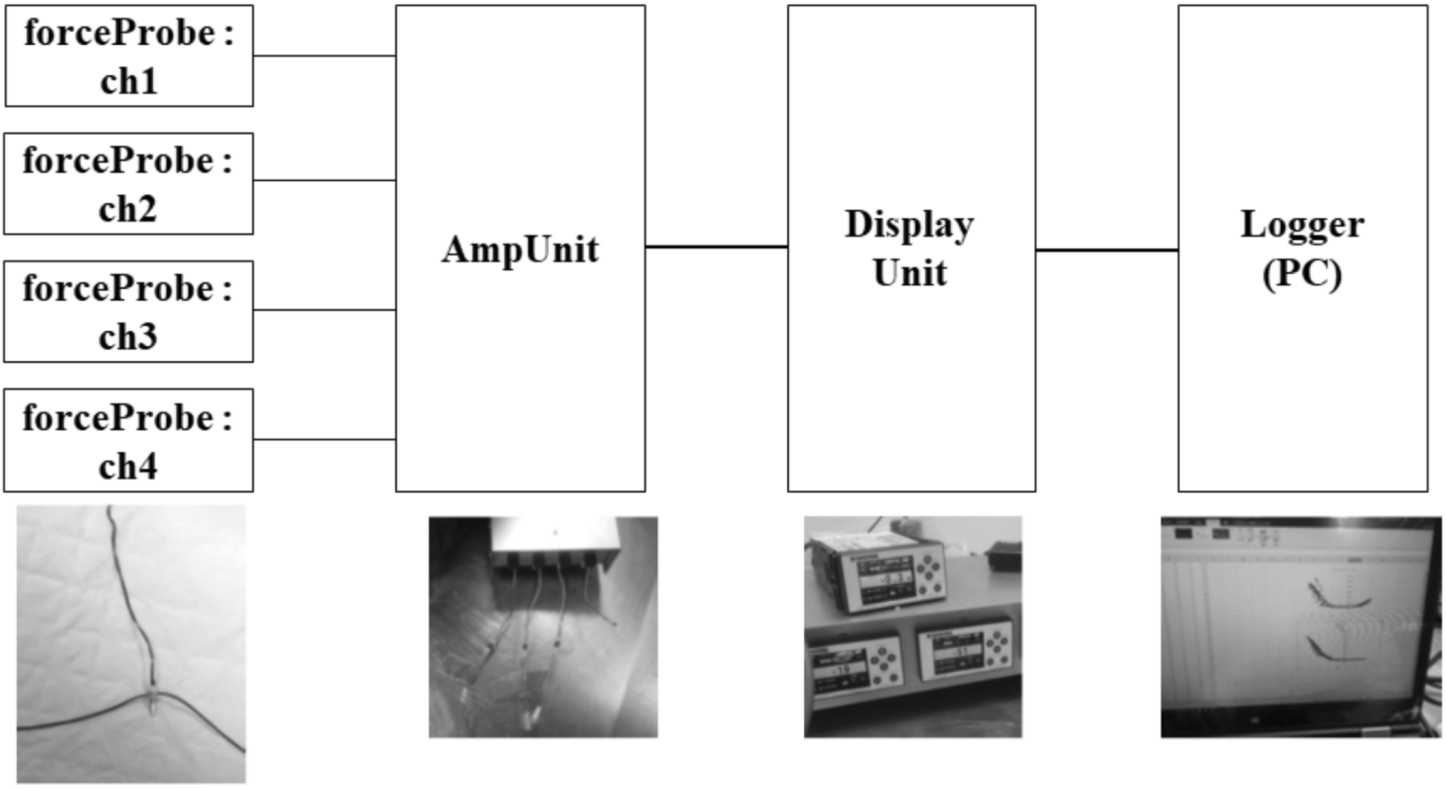

Figure 1

Figure 1

Miniaturization ligament performance probe system This is composed of a force probe (left), an amplifier unit (middle left), a display unit (middle right), and a logger (right).

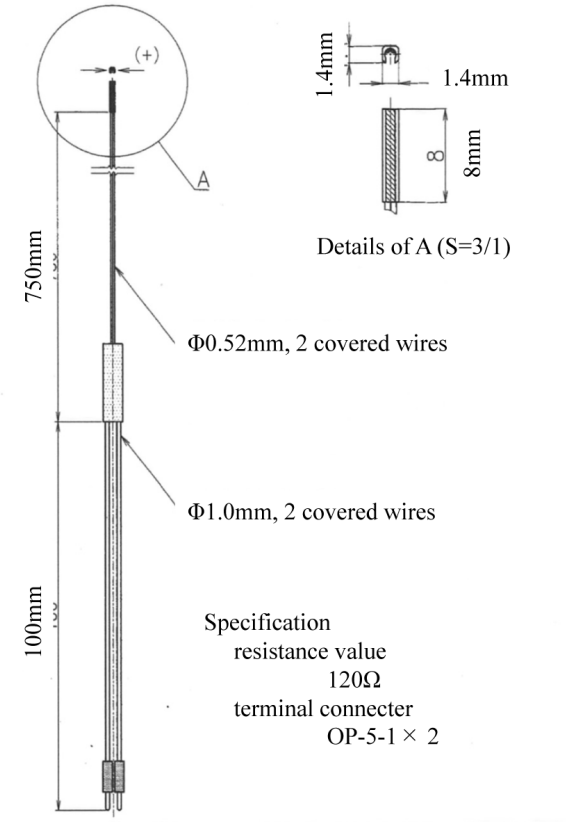

Figure 2A

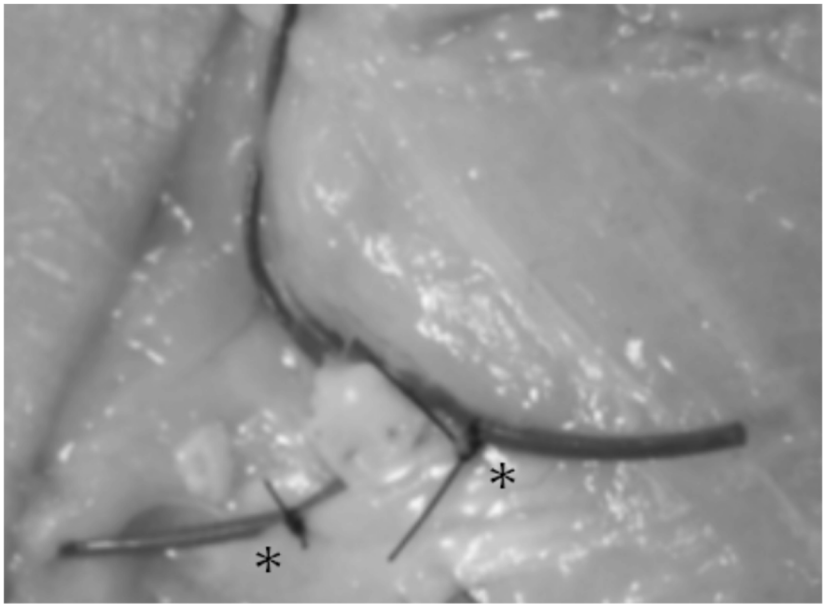

Figure 2B

Figure 2

Force probe (strain gauge) The force probe is rectangular shaped (Fig 2A) and has a tubular structure with slits entering vertically on one side of its surface (Fig 2B).

Figure 3

Figure 3

Setup of the specimen The lower limb is fixed vertically to the measurement desk using an Ilizarov ring–shaped external fixator, and a performance cube (*), clock (†) and an arm (‡) are affixed to an acrylic plate.

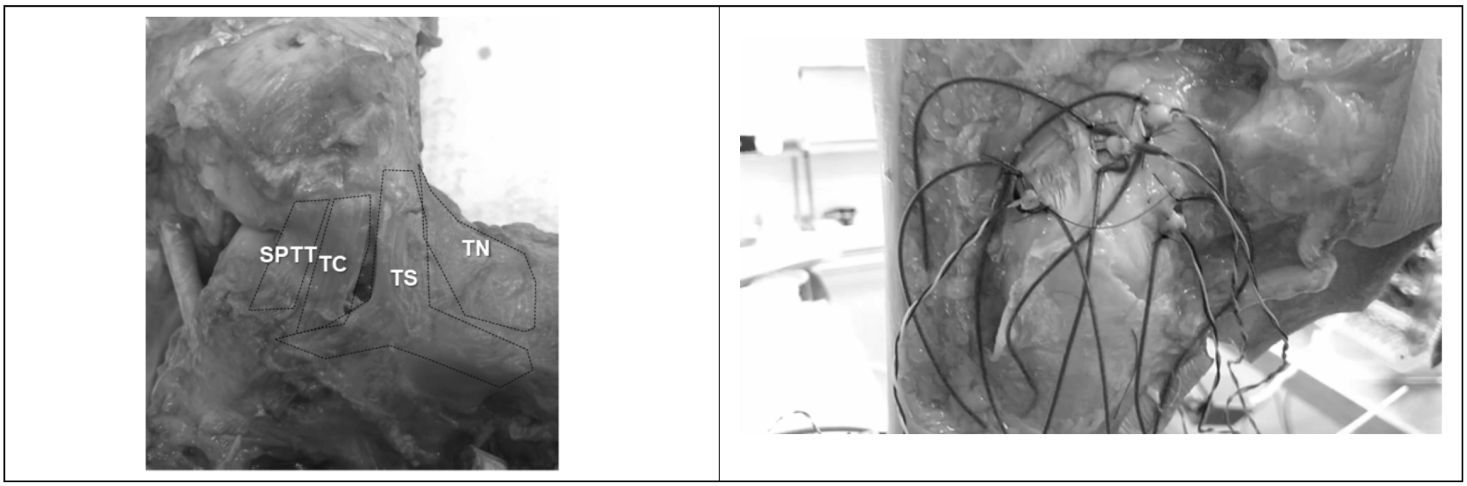

Figure 4A

Figure 4B

Figure 4

Trace each superficial deltoid ligament Figure 4A Each ligament was not isolated to investigate as one unit and the lines were drawn to connect the attachment to each bone tracing each ligament. Figure 4B A force probe was placed in the mid-substance of each ligamentous band of the TNL, TSL, TCL, and SPTTL such that the slit of the force probe was aligned with the long axis of the ligament fibres.

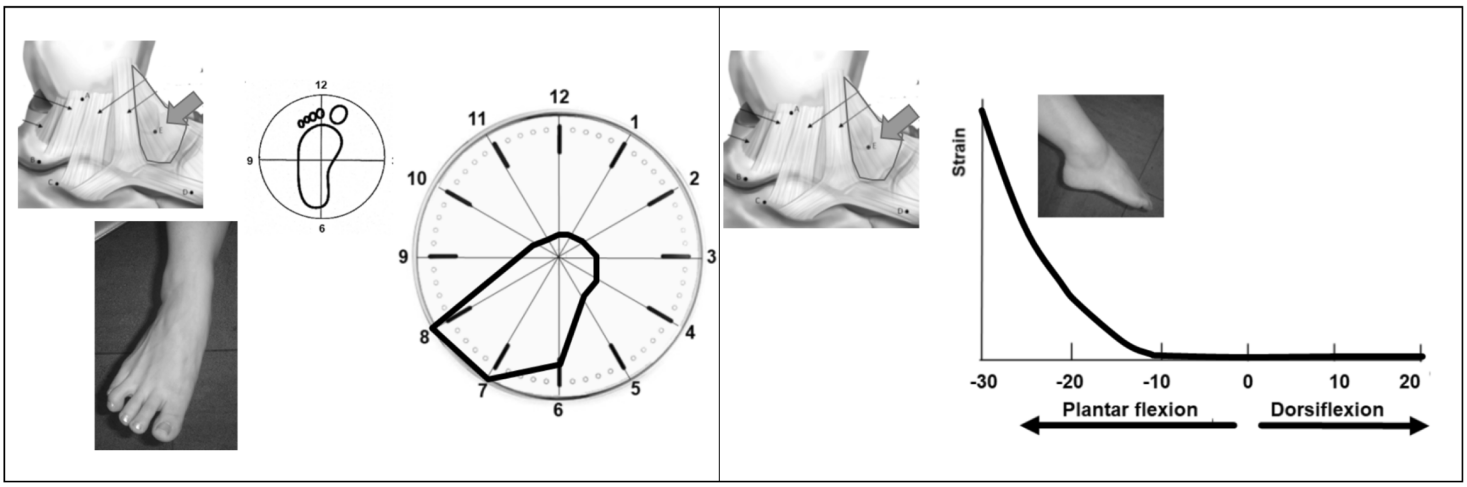

Figure 5A

Figure 5B

Figure 5

Strain pattern of tibionavicular ligament (TNL) Figure 5A The TNL worked most effectively in plantarflexion-abduction in clock motion. Figure 5B The TNL began to tense gradually at 10° plantarflexion. The tension became stronger as the plantarflexion angle increased in axial motion.

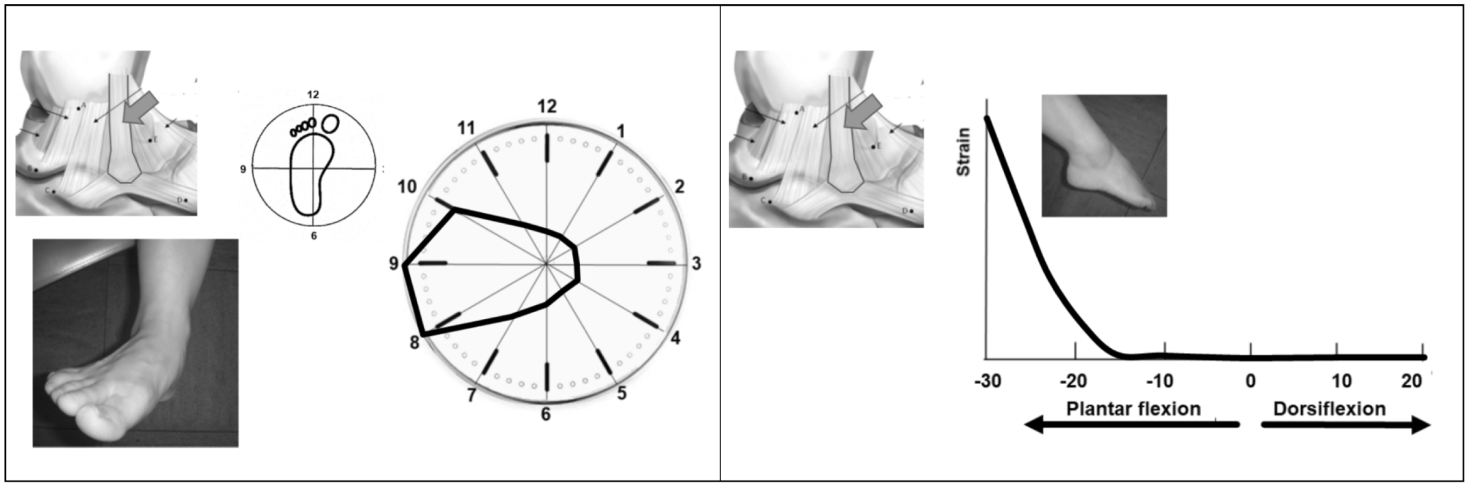

Figure 6A

Figure 6B

Figure 6

Strain pattern of tibiospring ligament Figure 6A The TSL worked most effectively in eversion. Figure 6B The TSL began to tense gradually at 15° plantarflexion and the tension became stronger as the angle increased.

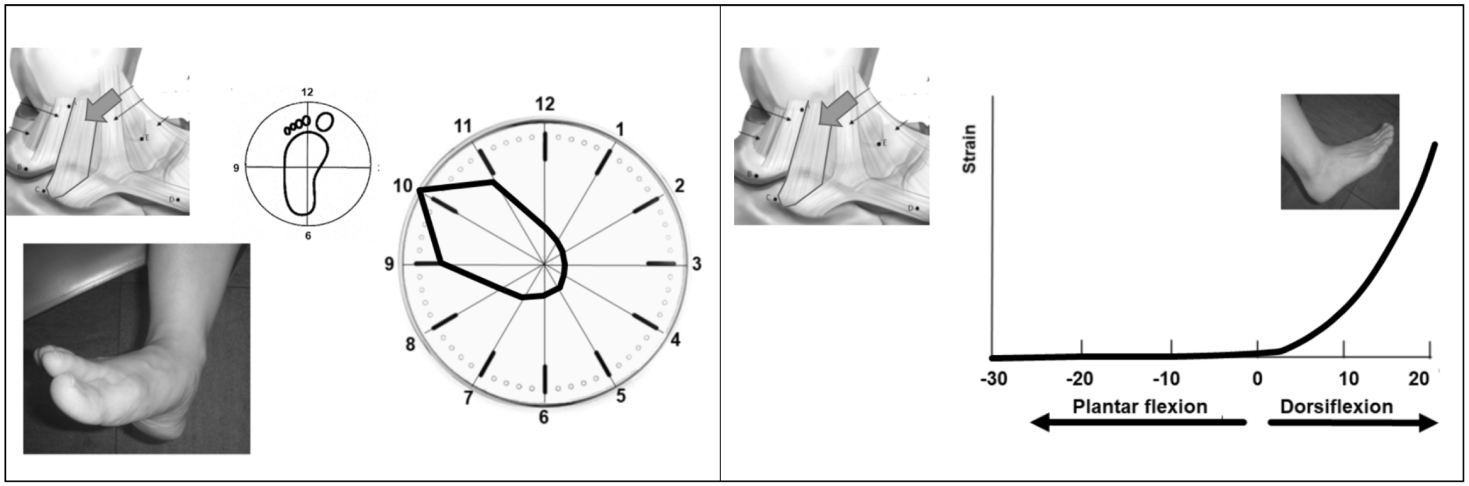

Figure 7A

Figure 7B

Figure 7

Strain pattern of tibiocalcaneal ligament Figure 7A The TCL worked most effectively in pronation. Figure 7B The TCL began to tense gradually at 0° dorsiflexion and the tension became stronger as the angle increased.

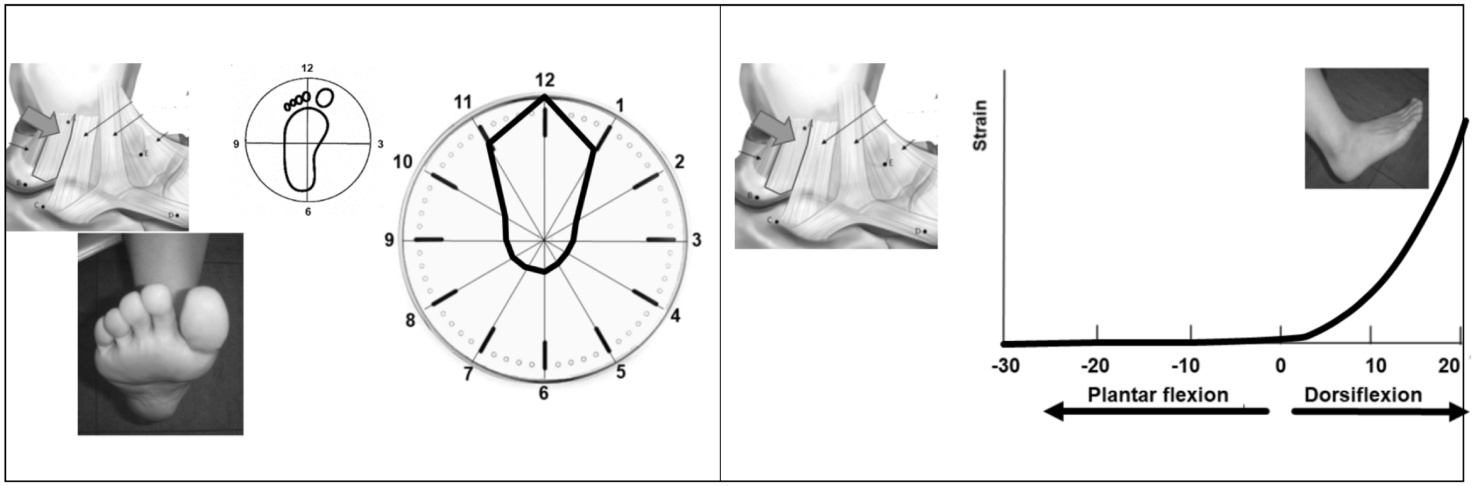

Figure 8A

Figure 8B

Figure 8

Strain pattern of superficial posterior tibiotalar ligament Figure 8A The SPTTL worked most effectively in dorsiflexion. Figure 8B The SPTTL began to tense gradually at 0° dorsiflexion. The tension became stronger as the angle increased.